ANL-6963

Argonne National Laboratory

ELECTRICAL END LOSSES IN AN MHD CHANNEL OF LINEARLY VARIABLE CROSS SECTION

by

Jerzy R. Moszynski

Printed in USA. Price $1.00. Available from the Clearinghouse for Federal Scientific and Technical Information, National Bureau of Standards, U. S. Department of Commerce, Springfield, Virginia

ANL-6963
Propulsion Systems and
Energy Conversion
(TID-4500, 40th Ed.)
AEC Research and
Development Report

ARGONNE NATIONAL LABORATORY
9700 South Cass Avenue
Argonne, Illinois 60440

ELECTRICAL END LOSSES IN AN MHD CHANNEL OF LINEARLY VARIABLE CROSS SECTION

by

Jerzy R. Moszynski

Reactor Engineering Division, ANL

and

Associated Midwest Universities

March 1965

Operated by The University of Chicago
under
Contract W-31-109-eng-38
with the
U. S. Atomic Energy Commission

FOREWORD

This report is one of a series that describes heat-transfer and fluid-flow studies performed at Argonne under a program sponsored jointly by the Associated Midwest Universities and the Argonne National Laboratory.

The earlier reports in this series are:

ANL-6625 Local Parameters in Cocurrent Mercury-Nitrogen Flow
L. G. Neal

ANL-6667 A Study of the Flow of Saturated Freon-11 through Apertures and Short Tubes
Hans K. Fauske and Tony C. Min

ANL-6674 Reduction of Vapor Carryunder in Simulated Boiling
P. L. Miller and C. P. Armstrong

ANL-6710 Transient Behavior of a Natural-Circulation Loop Operating Near the Thermodynamic Critical Point
Darrel G. Harden

ANL-6734 Two-phase (Gas-liquid) System: Heat Transfer and Hydraulics. An Annotated Bibliography
Robert R. Kepple and Thomas V. Tung

ANL-6738 Development of an Electrical Resistivity Probe for Void-fraction Measurements in Air-Water Flow
George P. Nassos

ANL-6754 An Experimental Investigation of Two-phase, Two-component Flow in a Horizontal, Converging-diverging Nozzle
Joseph A. Vogrin, Jr.

ANL-6755 Two-component Two-phase Flow Parameters for Low Circulation Rates
Georges E. Smissaert

ANL-6779 Two-phase Critical Flow with Application to Liquid-Metal Systems (Mercury, Cesium, Rubidium, Potassium, Sodium, and Lithium)
Hans K. Fauske

ANL-6796 The Slug-annular Flow Regime Transition at Elevated Pressure
Peter Griffith

ANL-6854 Effect of a Transverse Magnetic Field on Vertical Two-phase Flow through a Rectangular Channel
Richard J. Thome

ANL-6862 Two-phase Heat Transfer with Gas Injection through a Porous Boundary Surface
A. A. Kudirka

ANL-6948 Condensation of Metal Vapors: Mercury and the Kinetic Theory of Condensation
Donald J. Wilhelm

LIST OF FIGURES

No.	Title	Page
1.	Schematic Diagram of MHD Channel	8
2.	Generator Channel in Complex z-plane	9
3.	Generator Channel in Complex z'-plane	11
4.	Generator Channel in Complex w-plane	11
5.	Dimensionless Current and Power Developed	16
6.	Simplified Model of MHD Channel	17
7.	Comparison of Present Theory and Approximation of Ref. (4)	20
A-1.	Analog Models Used to Verify Approximate Calculation Procedure	22

LIST OF TABLES

No.	Title	Page
1.	Calculated Results	19
A-1.	Results of Analog Study	22

NOMENCLATURE

NOMENCLATURE

a,b,c	Constants
$\vec{B}$	Magnetic induction
B_0	Applied field
$\vec{E}$	Electric field intensity
h	Channel width in direction of current flow
h_1	Channel width at inlet
h_2	Channel width at exit
h_m	Log-mean width of generator channel, defined by Eq. (7)
I	Total current
I_e	End-loss current
$\vec{j}$	Current density
k	Argument of elliptic integral
K,K'	Complete elliptic integrals of the first kind
L	Length of generator channel
L_1,L_2	Lengths, defined by Eq. (33) and Fig. 6
$\vec{n}$	Unit vector normal to surface of an electrode
P_{el}	Power developed
P_i	Power developed in ideal channel
R_e	Equivalent resistance of end current loops
R_i	Internal resistance of channel
R_0	External load resistance
S	Surface of electrode
t	Time
U	Fluid velocity
U_1	Inlet fluid velocity
U_m	Mean fluid velocity
u	Integration variable
V	Electrode voltage
V_0	Induced emf
V_ℓ	Load electrode voltage
w,z,z'	Complex variables
W	Thickness of channel
α	Channel half-angle
β	Location of downstream electrode end in w-plane
μ_0	Magnetic permeability of free space
ν	Kinematic viscosity
η,η'	Voltage load-coefficients
ρ	Electrical surface resistivity
σ	Electrical conductivity
ϕ	Potential
ϕ_ℓ	Electrode potential
ψ	Electrical stream function

ELECTRICAL END LOSSES IN AN MHD CHANNEL OF LINEARLY VARIABLE CROSS SECTION

by

Jerzy R. Moszynski

ABSTRACT

The electrical losses due to end-shorting of electrodes in an MHD channel of linearly variable cross section have been calculated, under the assumption of large Reynolds number and small magnetic Reynolds number. It is shown that a simplified calculation procedure yields exact results and, further, that an approximate procedure, based on the results for a constant-area channel, provides satisfactory accuracy for channels of small included angle and/or relatively large aspect ratio.

I. INTRODUCTION

In an MHD generator channel of finite aspect ratio (finite ratio of length to width), the actual power density is less than the value calculated for a channel of infinite aspect ratio. This difference is due to current loops at the two ends of the channel. The net effect is one of providing between the electrodes a conduction path, which acts as a shunt resistance in parallel with the load. Thus, for a given load and generated emf, both the net load-current and the voltage load-coefficient are reduced.

The magnitude of the end losses in MHD channels of constant cross section have been calculated for various conditions by Sutton, Hurwitz, and Poritsky,[1] Shercliff,[2] Fishman,[3] and others. The critical importance of these losses is pointed out in Ref. (1), where it is shown that for sufficiently small aspect ratios, the operation of an MHD channel as a generator may become impossible.

The problem of end losses in an MHD channel of variable cross section does not appear to have received any attention in the published literature. However, a generator channel of variable cross section has been proposed recently for an MHD cycle, with either a single-phase or a two-phase fluid flowing through the channel.[4]

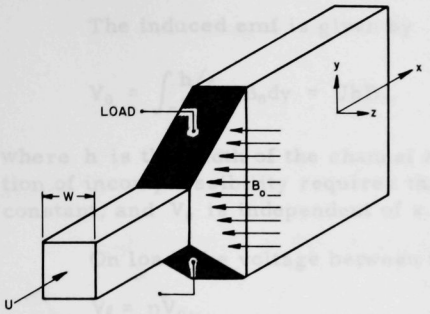

Fig. 1. Schematic Diagram of MHD Channel

This report is concerned with the problem of calculating the end losses in a channel of linearly varying cross section, as shown in Fig. 1. A single-phase, incompressible, conducting fluid flows in the x-direction through a duct of constant thickness W in the z-direction. The power generated is drawn off the electrodes, shown shaded.

The mathematical model of the generator and the general method of analysis are outlined first. The analysis is then applied to two specific cases. Subsequently, an approximate method is developed and is shown to yield exact results. Finally, a comparison is made with an earlier approximation.[4]

II. ANALYSIS

For the purposes of analysis, the following simplifying assumptions are made:

(1) The flow is one-dimensional, and viscous effects are neglected. This is apt to be valid for cases in which the Reynolds number UL/ν is large. Physically, this assumption may be applicable to turbulent flow of a liquid metal or, generally, to moderate-velocity flow of a plasma. The fluid is homogeneous and incompressible; this restricts the validity of the analysis to liquid metals or to low Mach-number gas flow.

(2) The applied magnetic field is steady, uniform, parallel to the z-axis, and applied only in the region of the variable cross-sectional area. This assumption neglects the usual lateral decay of a magnetic field. It is also assumed that the magnetic field induced by the load current can be neglected; this implies a low magnetic Reynolds number ($\mu_0 \sigma UL$), which may not be applicable in the case of a liquid metal in a relatively large duct.

(3) The electrodes are perfect conductors, while the channel walls both upstream and downstream of the electrodes are perfect insulators.

We write Ohm's law in the form:

$$\vec{j} = \sigma(\vec{E} + \vec{U} \times \vec{B}). \qquad (1)$$

The induced emf is given by

$$V_0 = \int_{-h/2}^{h/2} UB_0 dy = UhB_0, \tag{2}$$

where h is the width of the channel at the station considered. The assumption of incompressibility requires that UhW is constant; thus Uh is constant, and V_0 is independent of x.

On load, the voltage between the electrodes is given by

$$V_\ell = \eta V_0, \tag{3}$$

where η is the voltage load-coefficient.

As a result of assumption (2),

$$\partial \vec{B}/\partial t = 0,$$

we may put

$$\vec{E} = -\text{grad}\ \phi$$

and consider the electrodes to be at potentials ϕ_ℓ and $-\phi_\ell$, respectively; thus,

$$\phi_\ell = \frac{1}{2} V_\ell = \frac{1}{2} \eta V_0. \tag{4}$$

For present purposes, we are interested in the total current between the electrodes. To this end, we have to integrate $\vec{j} \cdot \vec{n}\, dS$ over the surface S of an electrode. Since $\vec{U} \times \vec{B}$ has only the component in the y-direction, given by Eq. (2), we obtain

$$I = \int_S \vec{j} \cdot \vec{n}\, dS = \sigma W \left\{ B_0 \int_{x_1}^{x_2} U(x) dx - \int_A^C \left(\frac{\partial \phi}{\partial y} dx - \frac{\partial \phi}{\partial x} dy \right) \right\}. \tag{5}$$

Here x_1 and x_2 denote, respectively, the values of the x-coordinate at the two ends of the electrode A and C, and the second integral is a line integral between A and C (see Fig. 2).

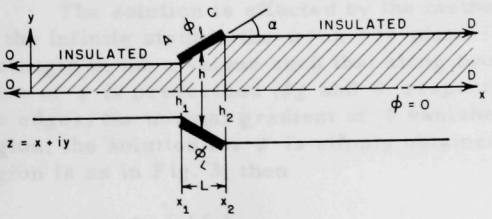

Fig. 2

Generator Channel in Complex z-plane

The first integral in Eq. (5) may be evaluated directly; that is,

$$\sigma W B_0 \int_{x_1}^{x_2} U(x)dx = \sigma W B_0 U_m L, \tag{6}$$

where

$$U_m h_m = U_1 h_1 = U_2 h_2 = U(x)h(x) = \text{const}$$

and

$$h_m = (h_2 - h_1)/\ln(h_2/h_1).$$

To evaluate the second integral on the right-hand side of Eq. (5), it is necessary to obtain a solution for the potential field ϕ between the electrodes. To this end, we must consider the geometry of the generator in somewhat more detail, particularly with respect to the region beyond the electrodes. With reference to Fig. 2, we need to consider only the upper half of the generator, because of symmetry.

The governing equation of the potential field is obtained by taking the divergence of Eq. (1) and is Laplace's equation,

$$\nabla^2\phi = 0. \tag{8}$$

Equation (8) is to be solved within the infinite strip shown shaded in Fig. 2, and subject to the following boundary conditions:

$$y = 0, \qquad \phi = 0 \text{ (by symmetry)}; \tag{9a}$$

$$y = h,\ x < x_1, \qquad \frac{\partial\phi}{\partial y} = 0 \text{ (insulated)}; \tag{9b}$$

$$y = h,\ x_1 \leq x \leq x_2, \qquad \phi = \phi_\ell \text{ (prescribed)}; \tag{9c}$$

$$y = h,\ x > x_2, \qquad \frac{\partial\phi}{\partial y} = 0 \text{ (insulated)}. \tag{9d}$$

The solution is effected by the method of conformal mapping, whereby the infinite strip in the $z = x + iy$ plane is eventually mapped into a rectangle in the z'-plane such that along two edges of the rectangle, the value of ϕ is prescribed (ϕ_ℓ and 0, respectively), while along the remaining two edges, the normal gradient of ϕ vanishes. In such a transformed region, the solution for ϕ is simply obtained, since if the transformed region is as in Fig. 3, then

$$\phi = -\phi_\ell\,(x'/a). \tag{10}$$

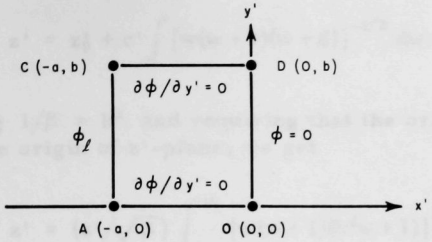

Fig. 3

Generator Channel in Complex z'-plane

The transformation is carried out in two stages. First, by considering the infinite strip as a doubly degenerate quadrilateral, we map it into the upper half of the $w = u + iv$ plane by means of the Schwarz-Christoffel transformation:

$$z = z_0 + c\int\left(\frac{w+1}{w+\beta}\right)^{\alpha/\pi}\frac{dw}{w}. \tag{11}$$

The positions of the vertices of the quadrilateral OACD in the w-plane are shown in Fig. 4. Since the constants z_0 and c are arbitrary, we are at liberty to fix the position of three of the vertices in the w-plane which, in turn, determines the three arbitrary elements of the two constants (z_0, modulus of c, and argument of c). In the present case, we choose the location of the vertices A, O, and D. The location of the vertex C in the w-plane must then be determined to facilitate the correct mapping of C into the z-plane.

Fig. 4

Generator Channel in Complex w-plane

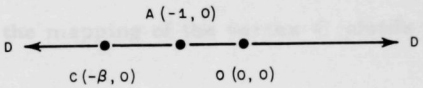

The procedure outlined above requires the explicit evaluation of the integral in Eq. (11); this does not appear to be possible except for selected values of α. Two cases will be considered in detail in Section III, but for the present, it will be assumed that the procedure has been carried out and the value of β determined. In general, the integrand in Eq. (11) is multivalued, and to describe the transformation completely, the branch must be specified. Further, one must expect β to depend on the half-angle α and on the linear dimensions of the generator. Thus $\beta = \beta(\alpha, L, h_1)$, or rather, $\beta = \beta(\alpha, L/h_1)$. Here L/h_1 plays the role of a modified aspect ratio.

The second step is the transformation of the upper half of the w-plane into the interior of the rectangle shown in Fig. 3, such that the four vertices in the z'-plane are O(0, 0), A(-a, 0), C(-a, b), and D(0, b). The general form of the required transformation is

$$z' = z'_0 + c' \int [w(w+1)(w+\beta)]^{-1/2}\, dw. \tag{12}$$

Letting $1/\beta = k^2$, and requiring that the origin of the w-plane be mapped into the origin of z'-plane, we get

$$z' = (c'/\sqrt{\beta}) \int_0^w [w(w+1)(k^2w+1)]^{-1/2}\, dw.$$

Considering next the mapping of the vertex A from the w-plane to the z'-plane, we get

$$z' = \frac{ia}{2K} \int_0^w [w(w+1)(k^2w+1)]^{-1/2}\, dw, \tag{13}$$

where

$$K(k) = \int_0^1 [(1-x^2)(1-k^2x^2)]^{-1/2}\, dx$$

is the complete elliptic integral of the first kind and is tabulated in the literature.[5,6] For convenience, a table of values of K is included as Appendix B.

Finally, consideration of the mapping of the vertex C yields the condition that

$$b/a = K'/K, \tag{14}$$

where

$$K'(k) = K(\sqrt{1-k^2}).$$

To complete the solution of our problem, we introduce an electrical stream function ψ which is defined by

$$\frac{\partial \psi}{\partial x} = \frac{\partial \phi}{\partial y}; \quad \frac{\partial \psi}{\partial y} = -\frac{\partial \phi}{\partial x}. \tag{15}$$

With the above substitution, the second integral on the right-hand side of Eq. (5) becomes

$$\int_A^C \frac{\partial \psi}{\partial y} dx - \frac{\partial \phi}{\partial x} dy = \int_A^C d\psi = \psi(C) - \psi(A). \tag{16}$$

In view of Eqs. (10) and (15), the expression for ψ in the z'-plane is simply

$$\psi = \phi_\ell(y'/a), \tag{17}$$

and

$$\psi(C) - \psi(A) = \phi_\ell(b/a) = \phi_\ell(K'/K). \tag{18}$$

Substituting Eqs. (6) and (18) into Eq. (5) and rearranging, we obtain, for the total current to the electrode,

$$I = \sigma W B_0 U_m L [1 - (\eta/2)(h_m/L)(K'/K)]. \tag{19}$$

The electrical power developed by the generator is given by

$$P_{el} = V_\ell I = \sigma \eta U_m^2 h_m B_0^2 W L [1 - (\eta/2)(h_m/L)(K'/K)]. \tag{20}$$

By differentiating Eq. (20) with respect to the loading factor η, we obtain for maximum power

$$\eta_{max\ P} = (L/h_m)(K/K'). \tag{21}$$

Further, we may compare the power developed with that developed by an idealized generator in which the sole component of the current is in the y-direction. Such a generator suffers no end losses, and the total power developed by it is given by

$$P_i = \eta'(1 - \eta')\sigma U_m^2 B_0^2 W L h_m. \tag{22}$$

The loading factors η and η', however, are not equal. It is shown in Ref. (4) that while the loading factor η' for the idealized generator is given by

$$\eta' = (R_i/R_0 + 1)^{-1}, \tag{23}$$

the loading factor η for a generator with end losses is given by

$$\eta = (1 + R_i/R_0 + R_i/R_e)^{-1}, \tag{24}$$

where R_e is the equivalent shunt resistance of the end loops in parallel with the load. From Kirchoff's Law, we have

$$V_0 - V_\ell = (I + I_e)R_i = (V_\ell/R_e + I)R_i,$$

and upon rearrangement,

$$I = (V_0/R_i)[1 - \eta(1 + R_i/R_e)].$$

It is easy to show that under the assumption of an idealized generator [e.g., Ref. (4)], the internal resistance is given by

$$R_i = h_m/(\sigma W L).$$

Thus, with the aid of Eq. (2),

$$I = \sigma U_m B_0 W L [1 - \eta(1 + R_i/R_e)]. \tag{25}$$

Comparison with Eq. (19) yields

$$\frac{R_i}{R_e} = \frac{1}{2}\frac{h_m}{L}\frac{K'}{K} - 1. \tag{26}$$

To evaluate the power loss due to end loops, it is necessary to compare (for a given generator and load) the ideal power given by Eq. (22) with the actual power given by Eq. (20), with the proviso that

$$1/\eta = 1/\eta' + R_i/R_e. \tag{27}$$

In Ref. (1), the power loss is computed on the assumption of equal electrode voltage with and without end losses. This requires that the external load resistance be different in the two cases.

The preceding analysis can only be carried out explicitly for specific angles α. For purposes of illustration, numerical results will be obtained in the next section. Subsequently, we shall demonstrate that an alternate method of calculation may be employed to yield exact results.

III. CALCULATION OF END LOSSES FOR SPECIFIC CASES

With reference to Eq. (11), the integrand may be transformed by the substitution:

$$(u)^{\pi/\alpha} = (w + 1)/(w + \beta).$$

After some rearrangement, this yields

$$\int \left(\frac{w+1}{w+\beta}\right)^{\alpha/\pi} \frac{dw}{w} = \int \frac{\pi}{\alpha}\left[\frac{1}{\beta(u)^{\pi/\alpha} - 1} + \frac{1}{1 - (u)^{\pi/\alpha}}\right] du. \tag{28}$$

For values of α such that π is an integral multiple of α, the above integral may be evaluated explicitly, although for $\pi/\alpha > 8$, the calculation may be quite laborious.

To appreciate better the magnitude of the end losses, consider the case of $\alpha = 45°$, which, while unlikely to be of a direct practical interest, permits a detailed calculation with a minimum of algebraic complications. In this case, we have, from Eq. (11),

$$z = z_0 + c\int\left(\frac{w+1}{w+\beta}\right)^{1/4}\frac{dw}{w} = \int 4\left(\frac{du}{1-u^4} + \frac{du}{\beta u^4 - 1}\right)$$

$$= z_0 + c\left[\ln\frac{1+u}{1-u} + 2\tan^{-1}u\right.$$

$$\left. + \frac{1}{\beta^{1/4}}\left(\ln\frac{\beta^{1/4}u - 1}{\beta^{1/4}u + 1} - 2\tan^{-1}\beta^{1/4}u\right)\right]. \qquad (29)$$

We are now free to locate the origin of the complex z-plane (see Fig. 2), and we choose it to coincide with the point A. Thus the required conditions are

$w = -1, \quad z = 0;$

$w = -\beta, \quad z = L(1+i);$

$w = +\infty, \quad z = +\infty - i(h_1/2);$

$w = -\infty, \quad z = +\infty + iL.$

When $w = 0$, the value of z depends on the direction from which the origin of the w-plane is approached. Thus, approaching along the real axis from the negative side ($w = 0_-$), $z = -\infty$; while approaching along the real axis from the positive side ($w = 0_+$), $z = -\infty - i(h_1/2)$.

Applying the first of the above conditions, we note that when $w = -1$, $u = 0$, and the first, second, and last terms in square brackets in Eq. (29) vanish. For small values of u, the phase of the logarithm in the third term is π, so that

$$z_0 = -ci\pi/\beta^{1/4}.$$

Considering next the condition at $w = 0_-$, we find that c must be real and positive, and from the condition at $w = 0_+$,

$$c = h_1\beta^{1/4}/2\pi;$$

therefore,

$$z_0 = -ih_1/2.$$

Finally, applying the condition at $w = -\beta$, we find

$$\beta = (2L/h_1 + 1)^4. \tag{30}$$

The remaining calculations indicated in Section II can now be carried out. The results for I and P_{el} may be reduced to a single plot shown in Fig. 5.

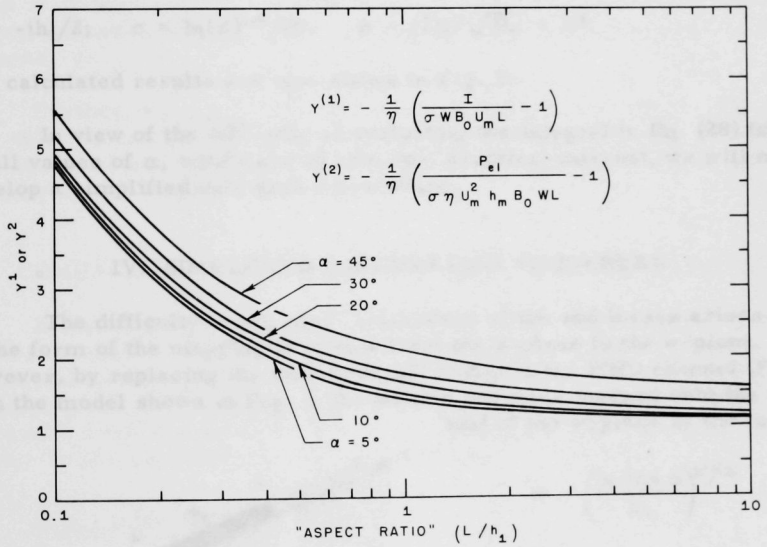

Fig. 5. Dimensionless Current and Power Developed

As a second illustration, consider the case of $\alpha = 30°$. We substitute

$$(w + 1)(w + \beta) = u^6,$$

and, after some algebraic operations, obtain

$$z = z_0 + c\left\{\ln\frac{1+u}{1-u} + \frac{1}{2}\ln\frac{1+u+u^2}{1-u+u^2} + \sqrt{3}\left(\tan^{-1}\frac{2u+1}{\sqrt{3}} + \tan^{-1}\frac{2u-1}{\sqrt{3}}\right)\right.$$

$$+ \frac{1}{(\beta)^{1/6}}\left[\ln\frac{(\beta)^{1/6}u - 1}{(\beta)^{1/6}u + 1} + \frac{1}{2}\ln\frac{(\beta)^{2/6}u^2 - (\beta)^{1/6}u + 1}{(\beta)^{2/6}u^2 + \beta^{1/6}u + 1}\right.$$

$$\left.\left. - \sqrt{3}\left(\tan^{-1}\frac{2(\beta)^{1/6}u + 1}{\sqrt{3}} + \tan^{-1}\frac{2(\beta)^{1/6}u - 1}{\sqrt{3}}\right)\right]\right\}.$$

Using the same methods as in the preceding examples, we obtain

$$z_0 = -ih_1/2; \quad c = h_1(\beta)^{1/6}/2\pi; \quad \beta = (2L/\sqrt{3h_1} + 1)^6. \tag{31}$$

The calculated results are also shown in Fig. 5.

In view of the difficulty of evaluating the integral in Eq. (28) for small values of α, which are of principal practical interest, we will next develop a simplified calculation procedure.

IV. SIMPLIFIED CALCULATION PROCEDURE

The difficulty in the exact calculation of the end losses arises out of the form of the mapping functions from the z-plane to the w-plane. However, by replacing the mathematical model of the MHD channel (Fig. 2) with the model shown in Fig. 6, the shaded region is mapped onto the upper half of the w-plane by the function

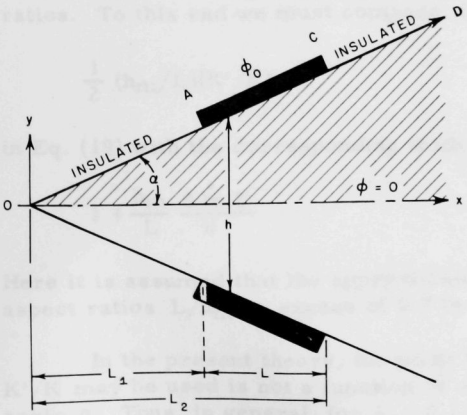

Fig. 6. Simplified Model of MHD Channel

$$w = \left(\frac{z\cos\alpha}{L_1}\right)^{\pi/\alpha} \tag{32}$$

with

$$\beta = (L_2/L_1)^{\pi/\alpha} \tag{33}$$

The transformation to the z'-plane and the subsequent calculations follow the path outlined in Section II. For a given channel of specified "aspect ratio" L/h_1 and angle α, the only difference in the calculated results obtained by the exact method and by the simplified procedure, outlined

above, can be due to a possibly different value of β, and hence k, obtained by the two methods.

While the geometry of Fig. 6 hardly resembles that of the actual channel (Fig. 2), one would expect the approximation to improve as the angle α decreases and/or as the "aspect ratio" increases. However, for α = 45 and 30°, the values of β obtained by the exact analysis [Eqs. (30) and (31), respectively] and given by Eq. (33) are identical.*

Although a rigorous proof that this must be the case for an arbitrary angle α appears to be difficult, one can argue heuristically as follows: since both Eq. (11) and Eq. (32) map the straight-line segment AC into a segment of the real axis in the w-plane, and since in both cases the location of A is the same (w = -1), the location of C must also be the same in both cases, and thus the value of β calculated by the two methods must be the same.

Further, since all these calculations yield results that are functions of β only, we can conclude that the simplified calculation procedure will yield exact results. Furthermore, this method can be employed without difficulty for all values of α.

V. COMPARISON WITH APPROXIMATE CALCULATION PROCEDURE

In Ref. (4), the end losses in MHD channels of variable cross section are computed by assuming an equivalent constant-area channel of width equal to the logarithmic-mean width (h_m) of the actual channel, and by applying the results of Ref. (1). To test the accuracy of this procedure, the results were compared for α = 5, 10, 20, and 30° over a range of aspect ratios. To this end we must compare, for example, the term

$$\frac{1}{2}(h_m/L)(K'/K)$$

in Eq. (19) with the corresponding term of the approximate theory:

$$1 + \frac{h_m}{L}\frac{2 \ln 2}{\pi}.$$

Here it is assumed that the approximation suggested by Sutton et al.[1] for aspect ratios L/h_m in excess of 0.7 is valid.

In the present theory, the point beyond which an approximation for K'/K may be used is not a function of only the aspect ratio but also of the angle α. Thus, in general, for $k < 0.1$ we may set

*This result at first appeared so startling that an analog study of the $\alpha = 30^\circ$ configuration was undertaken using "Teledeltos" conducting paper. This confirmed the analysis. The study is described briefly in Appendix A.

$$\frac{K'}{K} \approx \frac{4 \ln 2}{\pi} + \frac{1}{\alpha} \ln \frac{L_2}{L_1}. \tag{34}$$

The results of these calculations are presented in Table I and in Fig. 7. The agreement is very good, except for large half-angles α and small aspect ratios. In the latter case, the error may be due to the use of Sutton's approximation.

Table I

CALCULATED RESULTS

			$-\frac{1}{\eta}\left(\frac{I}{\sigma W B_0 U_m L} - 1\right)$	
L/h_1	k	K'/K	Present Theory	Ref. (4)
		$\alpha = 45°$		
0.1	0.694	1.016	5.573	NC[a]
0.25	0.444	1.364	3.364	NC
0.5	0.250	1.754	2.531	NC
1.0	0.111	2.281	2.076	NC
2.0	0.040	2.929	1.820	NC
3.0	NC	3.360[b]	1.726	NC
4.0	NC	3.680[b]	1.674	NC
5.0	NC	3.936[b]	1.641	NC
10.0	NC	4.759[b]	1.563	NC
		$\alpha = 30°$		
0.1	0.721	0.983	5.180	5.653
0.25	0.493	1.291	2.938	2.889
0.5	0.255	1.742	2.196	2.118
1.0	0.102	2.334	1.756	1.664
2.0	0.028	3.167	1.528	1.426
3.0	0.011	3.742	1.444	1.341
4.0	NC	4.179[b]	1.397	1.295
5.0	NC	4.526[b]	1.366	1.266
10.0	NC	5.714[b]	1.304	1.201
		$\alpha = 20°$		
0.1	0.729	0.972	4.923	5.553
0.25	0.520	1.250	2.869	3.022
0.5	0.247	1.762	2.066	2.033
1.0	0.086	2.443	1.626	1.586
2.0	0.021	3.335	1.415	1.374
3.0	NC[a]	4.189[b]	1.317	1.277
4.0	NC	4.685[b]	1.250	1.235
5.0	NC	5.175[b]	1.228	1.208
10.0	NC	6.937[b]	1.195	1.152

Table I (Contd.)

L/h_1	k	K'/K	$-\frac{1}{\eta}\left(\frac{I}{\sigma W B_0 U_m L} - 1\right)$ Present Theory	Ref. (4)
		$\alpha = 10°$		
0.1	0.738	0.960	4.885	5.483
0.25	0.469	1.326	2.768	2.839
0.5	0.311	1.611	1.749	1.957
1.0	0.067	2.594	1.414	1.514
2.0	0.010	3.812	1.260	1.291
3.0	NC	5.018[b]	1.226	1.215
4.0	NC	5.924[b]	1.187	1.177
5.0	NC	6.707[b]	1.154	1.152
10.0	NC	9.535[b]	1.113	1.093
		$\alpha = 5°$		
0.1	0.723	0.968	4.883	5.446
0.25	0.463	1.335	2.731	2.803
0.5	0.221	1.836	1.915	1.919
1.0	0.055	2.729	1.481	1.478
2.0	NC[a]	4.320[b]	1.260	1.257
3.0	NC	5.615[b]	1.186	1.182
4.0	NC	6.961[b]	1.148	1.145
5.0	NC	8.084[b]	1.125	1.123
10.0	NC	12.473[b]	1.078	1.076

[a]Not calculated.
[b]Calculated using Eq. (34).

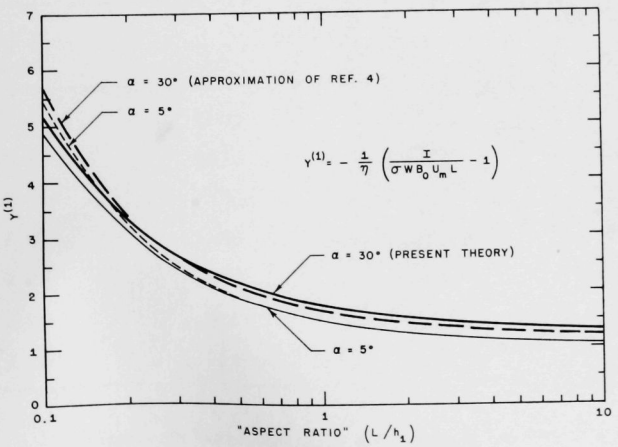

Fig. 7
Comparison of Present Theory and Application of Ref. (4).

VI. CONCLUSIONS

An exact calculation procedure for the end losses in an MHD channel of linearly variable cross section has been developed under the assumption of one-dimensional fluid flow. A simplified calculation procedure has yielded exact results, while the approximate method of Ref. (4) has been of acceptable accuracy. Since, however, the present procedure is simple to use, little is to be gained by the use of the approximate method of Ref. (4).

To use the present method for a given MHD channel, the following steps are necessary:

(1) Compute β from $\beta = (L_2/L_1)^{\pi/\alpha}$.

(2) Compute k from $k = 1/\sqrt{\beta}$.

(3) If $k > 0.1$, compute K(k) and $K' = K(\sqrt{1 - k^2})$ from Appendix B. If $k < 0.1$, compute K'/K from Eq. (34).

(4) Compute R_i/R_e from Eq. (26).

(5) Compute η from Eq. (24).

(6) Compute I and P_{el} from Eqs. (19) and (20), respectively.

APPENDIX A

Analog Study of Channel Configuration with $\alpha = 30°$

"Teledeltos" conducting paper with specific surface resistance $\rho = 2000\Omega$ was used in configurations as shown in Fig. A-1.

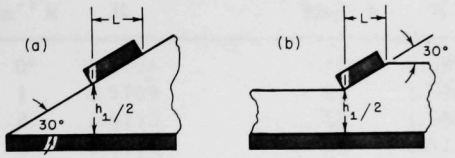

Fig. A-1

Analog Models Used to Verify Approximate Calculation Procedure

The electrodes, shown by thick lines, consisted of copper bars (1/4-in. square cross section) pressed firmly to the edge of the paper. The lateral extent of the paper was chosen such that further addition produced no noticeable difference in results. In both cases, the dimension L was constant at 5.2 in.

It can easily be shown that the resistance between the electrodes should be given by $(K/K')\rho$. The results of the study are summarized in Table A-1. It will be noticed that for the same minimum width the resistances measured for cases (a) and (b) are in agreement well within the experimental accuracy. Similarly, the agreement between calculated and measured resistances is satisfactory.

Table A-1

RESULTS OF ANALOG STUDY

$h_1/2$, in.	R_{meas}, ohm (a)	R_{meas}, ohm (b)	k	R_{calc}, ohm
12.4	1600	1600	0.520	1600
10.0	1450	1450	0.455	1490
8.0	1350	1400	0.383	1360
6.0	1300	1300	0.295	1260
4.0	1150	1100	0.186	1020
2.06	900	1000	0.0675	770
1.06	700	700	0.0166	570

This was intended only as a rough check, and no effort was made to eliminate the possibly large resistance between the paper and the electrodes.

APPENDIX B

Complete Elliptic Integrals

Note: Values of K for $\sin^{-1} k$ = 85 to 89° by 0.1°, and 89 to 90° by minutes

$\sin^{-1} k$	K	$\sin^{-1} k$	K	$\sin^{-1} k$	K
0°	1.5708	30°	1.6858	60°	2.1565
1	1.5709	31	1.6941	61	2.1842
2	1.5713	32	1.7028	62	2.2132
3	1.5719	33	1.7119	63	2.2435
4	1.5727	34	1.7214	64	2.2754
5	1.5738	35	1.7312	65	2.3088
6	1.5751	36	1.7415	66	2.3439
7	1.5767	37	1.7522	67	2.3809
8	1.5785	38	1.7633	68	2.4198
9	1.5805	39	1.7748	69	2.4610
10	1.5828	40	1.7868	70	2.5046
11	1.5854	41	1.7992	71	2.5507
12	1.5882	42	1.8122	72	2.5998
13	1.5913	43	1.8256	73	2.6521
14	1.5946	44	1.8396	74	2.7081
15	1.5981	45	1.8541	75	2.7681
16	1.6020	46	1.8691	76	2.8327
17	1.6061	47	1.8848	77	2.9026
18	1.6105	48	1.9011	78	2.9786
19	1.6151	49	1.9180	79	3.0617
20	1.6200	50	1.9256	80	3.1534
21	1.6252	51	1.9539	81	3.2553
22	1.6307	52	1.9729	82	3.3699
23	1.6365	53	1.9927	83	3.5004
24	1.6426	54	2.0133	84	3.6519
25	1.6490	55	2.0347	85	3.8317
26	1.6557	56	2.0571	86	4.0528
27	1.6627	57	2.0804	87	4.3387
28	1.6701	58	2.1047	88	4.7427
29	1.6777	59	2.1300	89	5.4349
				90	∞

$\sin^{-1} k$	K	$\sin^{-1} k$	K
85.0°	3.832	89° 0'	5.435
85.1	3.852	89 2	5.469
85.2	3.872	89 4	5.504
85.3	3.893	89 6	5.540
85.4	3.914	89 8	5.578
85.5	3.936	89 10	5.617
85.6	3.958	89 12	5.658
85.7	3.981	89 14	5.700
85.8	4.004	89 16	5.745
85.9	4.028	89 18	5.791
86.0	4.053	89 20	5.840
86.1	4.078	89 22	5.891
86.2	4.104	89 24	5.946
86.3	4.130	89 26	6.003
86.4	4.157	89 28	6.063
86.5	4.185	89 30	6.128
86.6	4.214	89 32	6.197
86.7	4.244	89 34	6.271
86.8	4.274	89 36	6.351
86.9	4.306	89 38	6.438
87.0	4.339	89 40	6.533
87.1	4.372	89 41	6.584
87.2	4.407	89 42	6.639
87.3	4.444	89 43	6.696
87.4	4.481	89 44	6.756
87.5	4.520	89 45	6.821
87.6	4.562	89 46	6.890
87.7	4.603	89 47	6.964
87.8	4.648	89 48	7.044
87.9	4.694	89 49	7.131
88.0	4.743	89 50	7.226
88.1	4.794	89 51	7.332
88.2	4.848	89 52	7.449
88.3	4.905	89 53	7.583
88.4	4.965	89 54	7.737
88.5	5.030	89 55	7.919
88.6	5.099	89 56	8.143
88.7	5.173	89 57	8.430
88.8	5.253	89 58	8.836
88.9	5.340	89 59	9.529
89.0	5.435	90 0	∞

REFERENCES

1. G. W. Sutton, H. Hurwitz, Jr., and H. Poritsky, Electrical and Pressure Losses in a Magnetohydrodynamic Channel Due to End Current Loops, Trans. AIEE, Part I: Communications and Electronics 80, No. 58 (1961) pp. 687-695.

2. A. Shercliff, Theory of Electromagnetic Flow Measurement, Cambridge University Press, Cambridge (1962).

3. F. Fishman, End Effects in Magnetohydrodynamic Channel Flow, Avco Corp.-Everett Research Laboratory, Everett, Massachusetts (Res. Note 135), AFBMD-TN-59-5 (June 1959).

4. M. Petrick and K. Y. Lee, Liquid MHD Power Cycle Studies, ANL-6954 (to be published).

5. Handbook of Chemistry and Physics, 34th edition, Chemical Rubber Publishing Co., Cleveland, Ohio (1952), pp. 234-235.

6. E. Jahnke and F. Emde, Tables of Functions with Formulae and Curves, Dover Publications, New York, N. Y. (1945).

REFERENCES